

## *Supporting Information*

# Nanoporous hexagonal TiO<sub>2</sub> superstructure as a multifunctional material for energy conversion and storage

*Eun Joo Lee,<sup>†,§</sup> Inho Nam,<sup>‡,§</sup> Jongheop Yi,<sup>‡,\*</sup> Jin Ho Bang<sup>†,§,\*</sup>*

<sup>†</sup>Department of Bionanotechnology, Hanyang University, 55 Hanyangdaehak-ro, Sangnok-gu, Ansan, Kyeonggi-do 426-791, South Korea, <sup>‡</sup>WCU Program of Chemical Convergence for Energy & Environment, School of Chemical and Biological Engineering, Institute of Chemical Processes, Seoul National University, Seoul 151-742, South Korea, <sup>§</sup>Department of Chemistry and Applied Chemistry, Hanyang University, 55 Hanyangdaehak-ro, Sangnok-gu, Ansan, Kyeonggi-do 426-791, South Korea.

<sup>§</sup>These authors contributed equally to this work.

**KEYWORDS.** Hexagonal TiO<sub>2</sub> superstructure, grain growth mechanism, nano-pores, dye-sensitized solar cells, lithium ion batteries

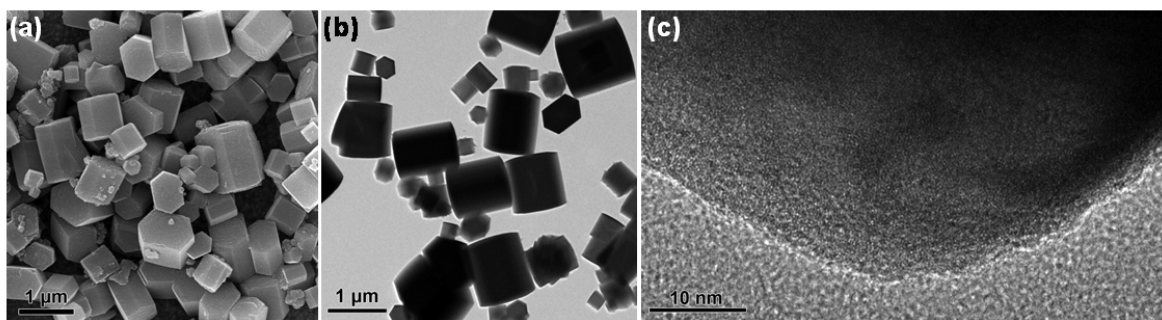


**Fig. S1** (a) SEM and (b and c) TEM images of HTO.

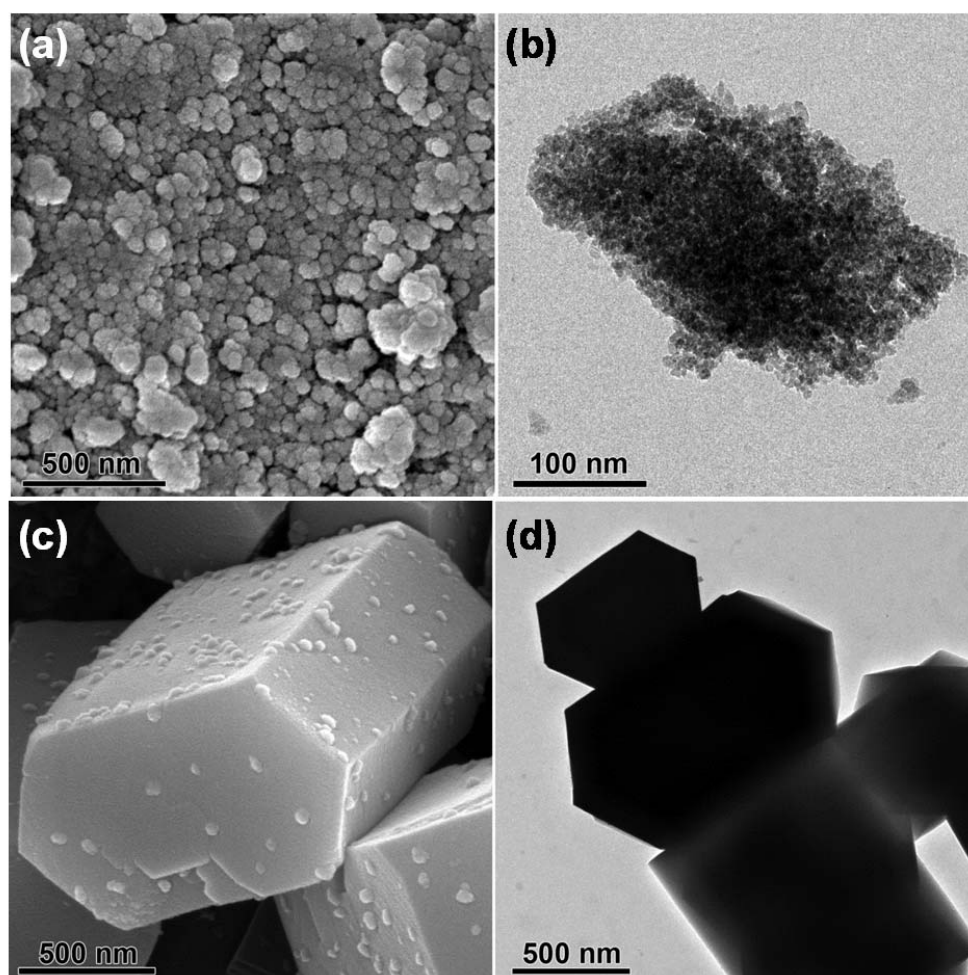


**Fig. S2** (a) SEM and (b) TEM images of  $\text{TiO}_2$  precursor prepared without oxalic acid (OA) and (c) SEM and (d) TEM images of  $\text{TiO}_2$  precursor prepared without sodium dodecyl benzene sulfonate (SBDS).

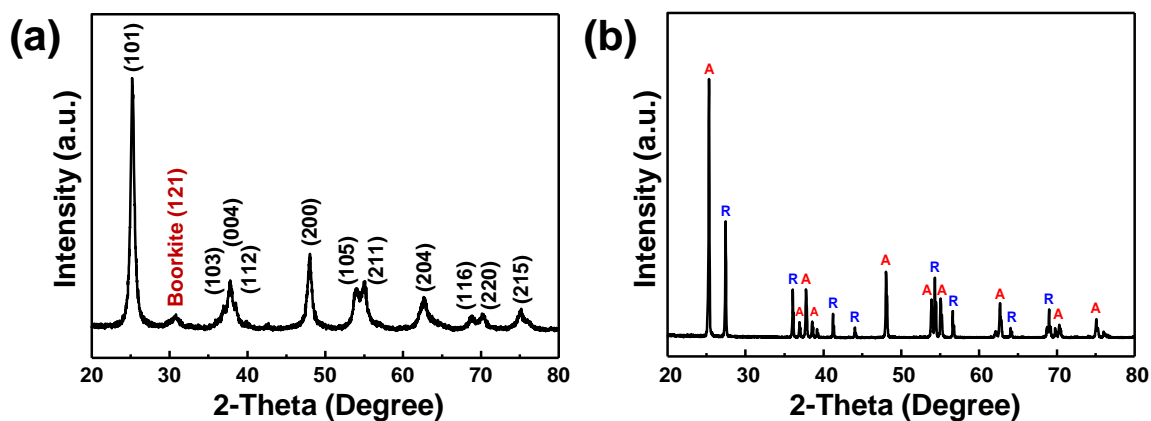


**Fig. S3** XRD pattern of (a) anatase/brookite TiO<sub>2</sub> obtained when HTO powder was directly transferred to a furnace held at 450 °C and annealed for 5 h and (b) anatase/rutile TiO<sub>2</sub> obtained when HTO powder was annealed at 900 °C for 5 h.

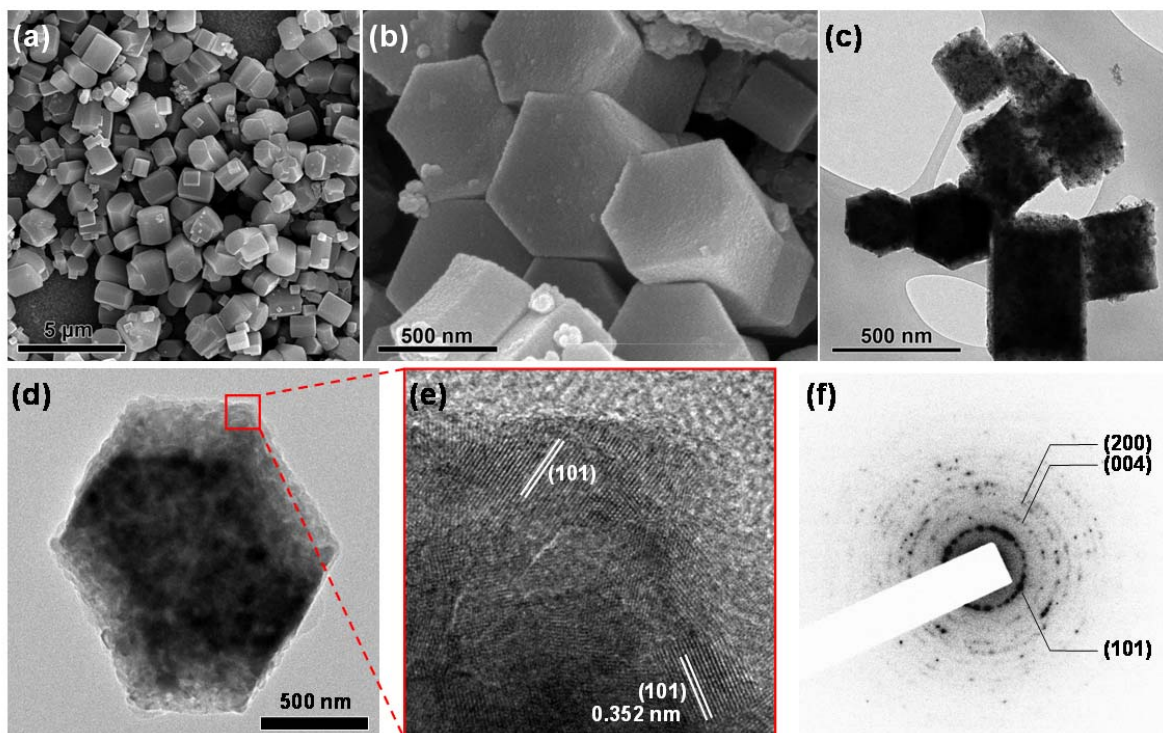


**Fig. S4** (a and b) SEM and (c-e) TEM images of HTS obtained by calcining HTO, and (f) its selected-area electron diffraction (SAED) patterns.

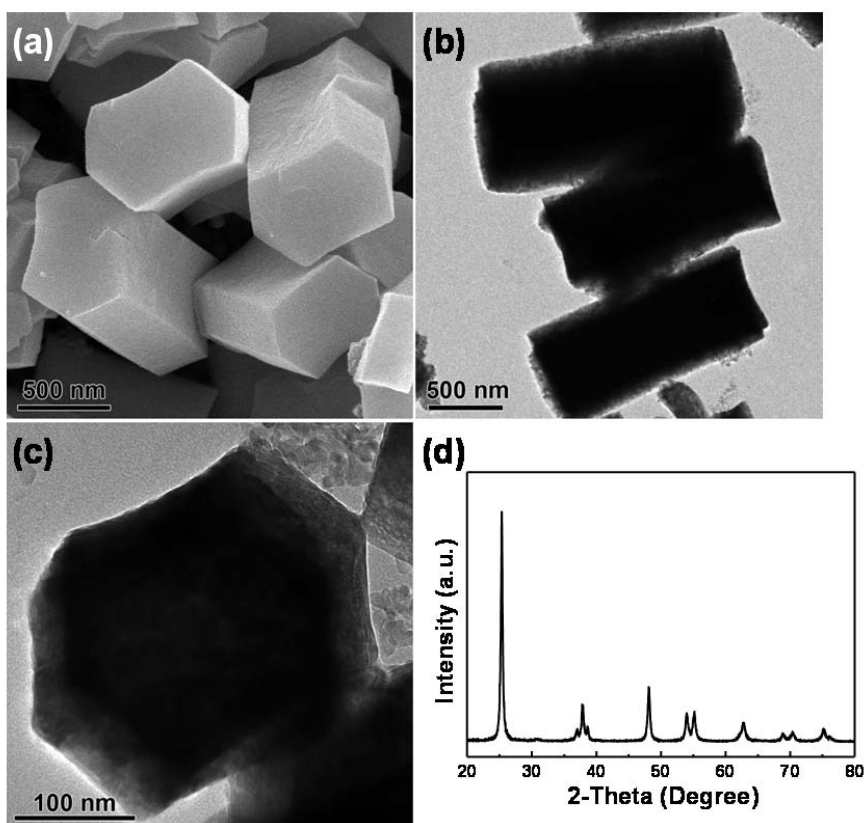


**Fig. S5** (a) SEM and (b) TEM images of TiO<sub>2</sub> obtained by calcining the TiO<sub>2</sub> precursor prepared without sodium dodecyl benzene sulfonate (SBDS), (c) XRD pattern of TiO<sub>2</sub> obtained by calcining the TiO<sub>2</sub> precursor prepared without sodium dodecyl benzene sulfonate (SBDS).

**Table S1.** Solar Cell Parameters of DSSCs with Various TiO<sub>2</sub> Films.

TiO <sub>2</sub> films	J <sub>sc</sub> (mA cm <sup>-2</sup> )	V <sub>oc</sub> (V)	FF	η (%)
NT/HTS	18.0	0.74	0.57	7.6
NT only	16.0	0.73	0.56	6.4
NT/DSL	16.7	0.73	0.56	6.8

**Table S2.** Solar Cell Parameters of DSSCs with TiO<sub>2</sub> Film of NT/HTS from multiple cell measurements.

NT/HTS	J <sub>sc</sub> (mA/cm <sup>2</sup> )	V <sub>oc</sub> (V)	FF	Eff (%)
Cell 1	18.0	0.737	0.570	<b>7.58</b>
Cell 2	18.2	0.741	0.555	7.48
Cell 3	17.6	0.737	0.575	7.44

**Table S3.** Solar Cell Parameters of DSSCs with TiO<sub>2</sub> Film of NT only from multiple cell measurements.

NT only	J <sub>sc</sub> (mA/cm <sup>2</sup> )	V <sub>oc</sub> (V)	FF	Eff (%)
Cell 1	16.0	0.732	0.558	<b>6.44</b>
Cell 2	16.1	0.722	0.570	6.61
Cell 3	15.9	0.707	0.565	6.33

**Table S4.** Solar Cell Parameters of DSSCs with TiO<sub>2</sub> Film of NT/DSL from multiple cell measurements.

NT/DSL	J <sub>sc</sub> (mA/cm <sup>2</sup> )	V <sub>oc</sub> (V)	FF	Eff (%)
Cell 1	16.7	0.725	0.562	<b>6.81</b>
Cell 2	16.5	0.725	0.567	6.79
Cell 3	16.3	0.731	0.584	6.94

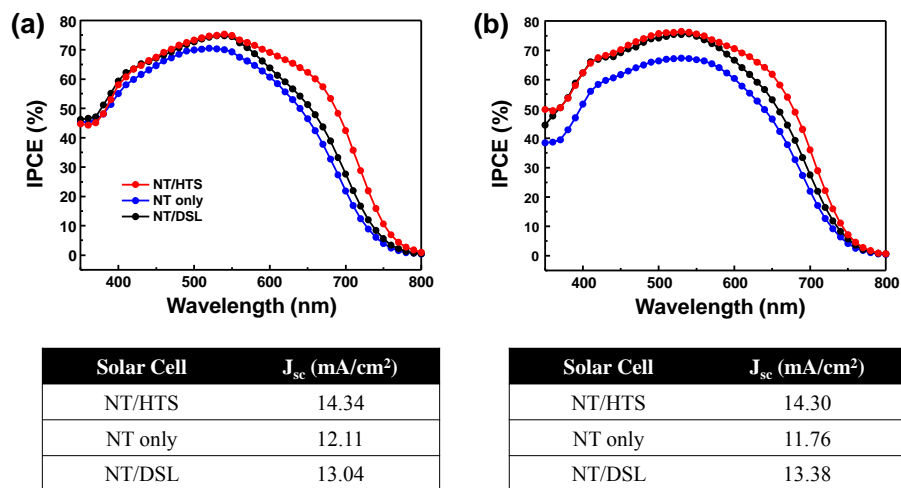


**Fig. S6** IPCE curves of DSSCs with different photoanodes from multiple measurements and photocurrent obtained by integration of IPCE spectra. Note that the integrated J<sub>sc</sub> values from the IPCE measurements are lower than those from J-V curve measurement because of mismatch in area and shape between excitation beam (rectangle: 0.1 cm×0.7 cm) and active area of solar cells (circle with 0.5 cm in diameter). Thus, some of photons from the excitation did not reach the active area during IPCE measurements.

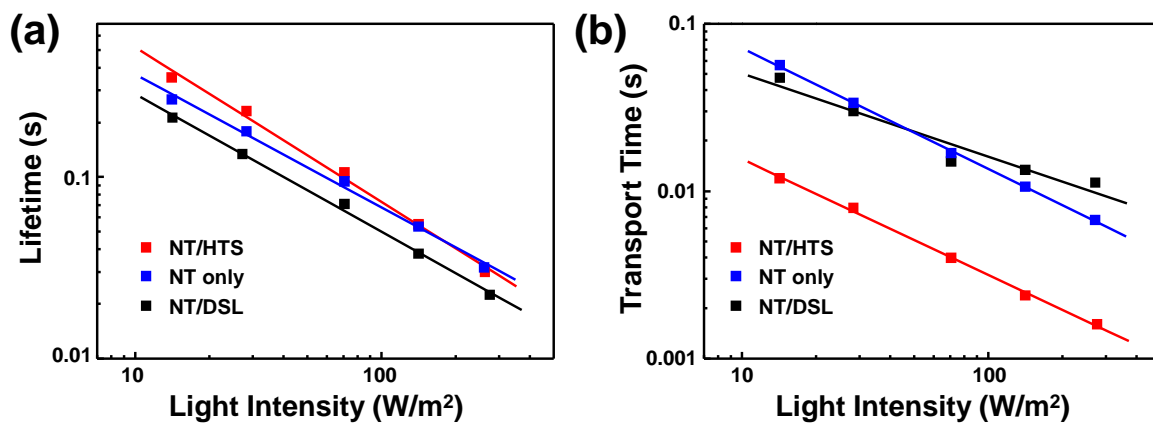


**Fig. S7** (a) Electron lifetime and (b) electron transport time as a function of light intensity for DSSCs with different TiO<sub>2</sub> layers.

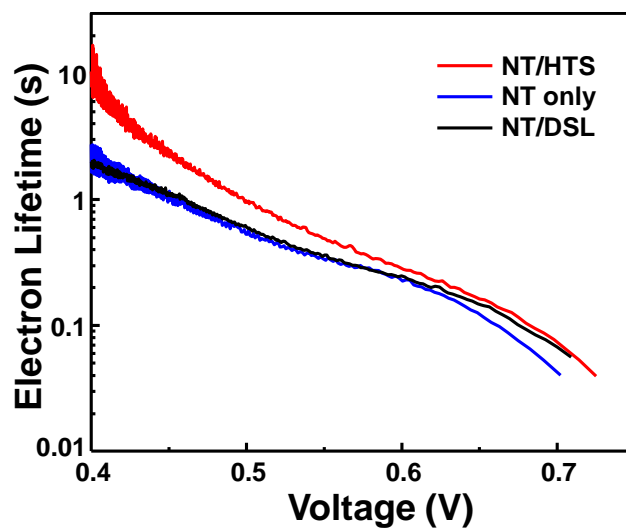


**Fig. S8** Electron lifetimes of DSSCs with different TiO<sub>2</sub> layers obtained from photovoltage decay measurement.

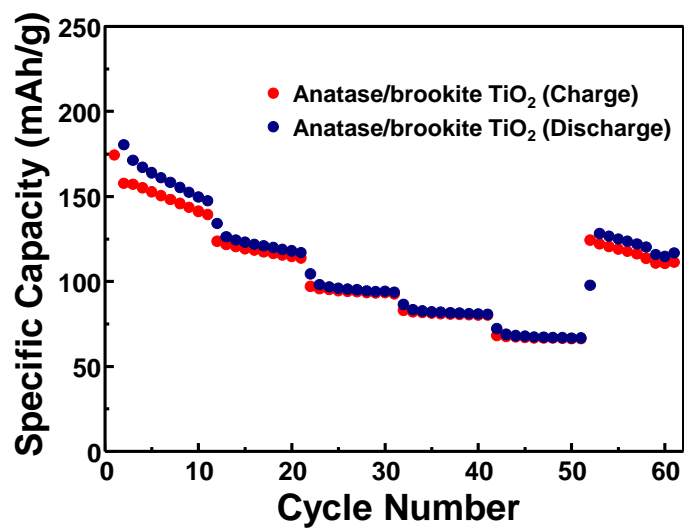


**Fig. S9** Specific capacities of anatase/brookite  $\text{TiO}_2$  at various C rates.

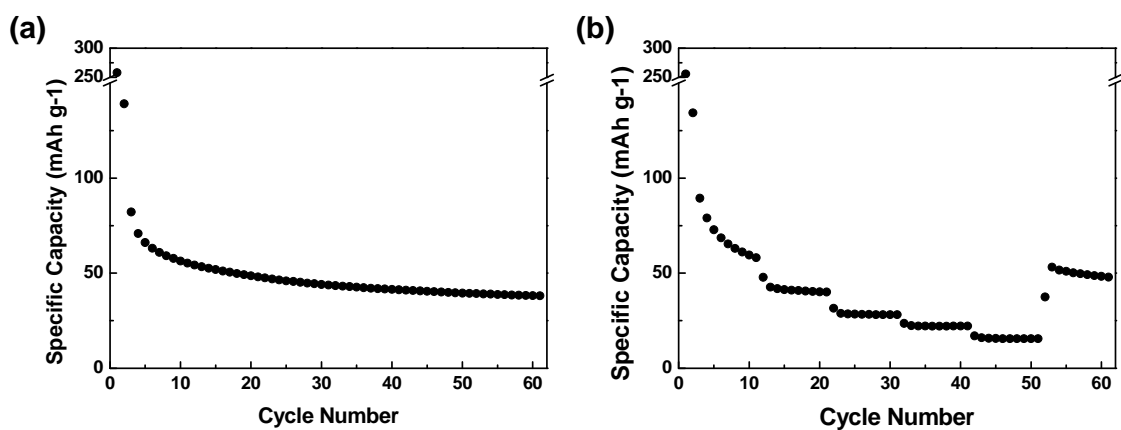


**Fig. S10** (a) Specific capacities of P25 anodes at 0.5 C during the first 100 galvanostatic cycles and (b) specific capacities of P25 cycled at various C-rates (0.5, 1, 2, 3, 5, and 0.5 C).



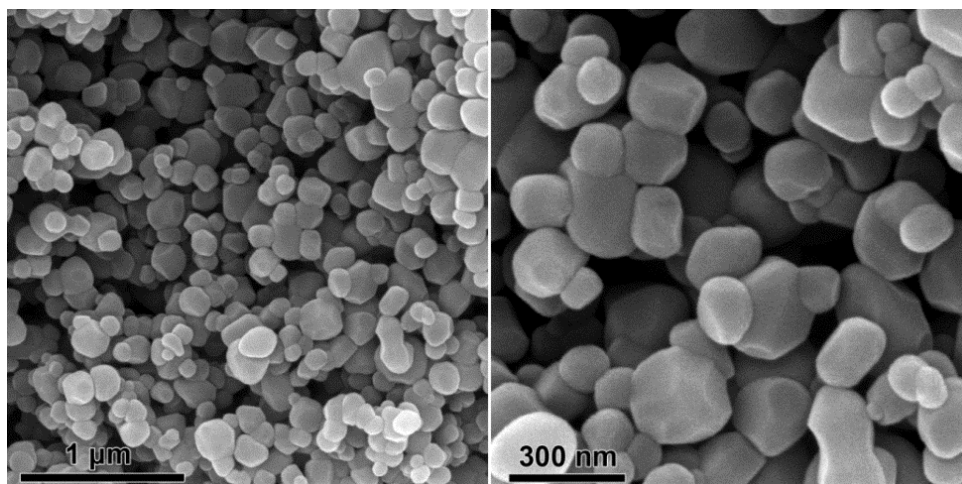


**Fig. S11** SEM images of C-TiO<sub>2</sub> (anatase, Sigma-Aldrich).

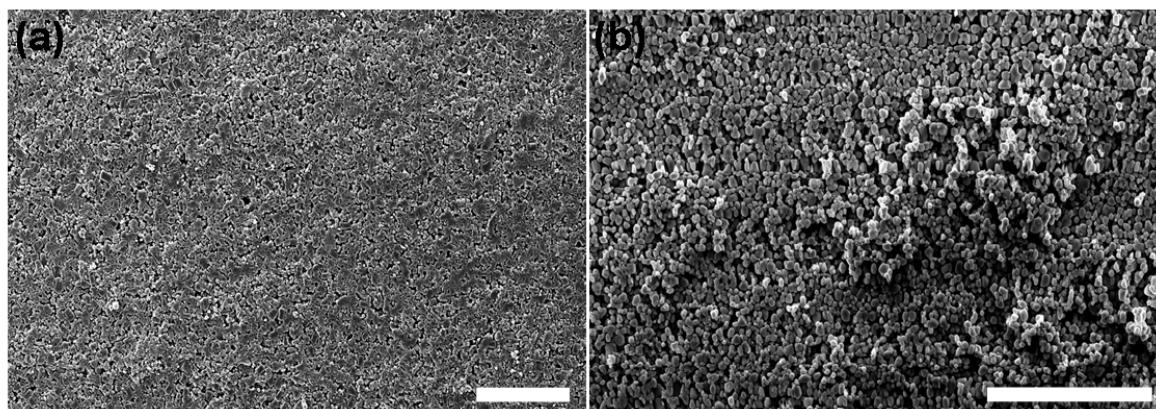


**Fig. S12** SEM images of (a) pelletized HTS and (b) pelletized conventional anatase TiO<sub>2</sub> spheres. Scale bar is 10 μm.

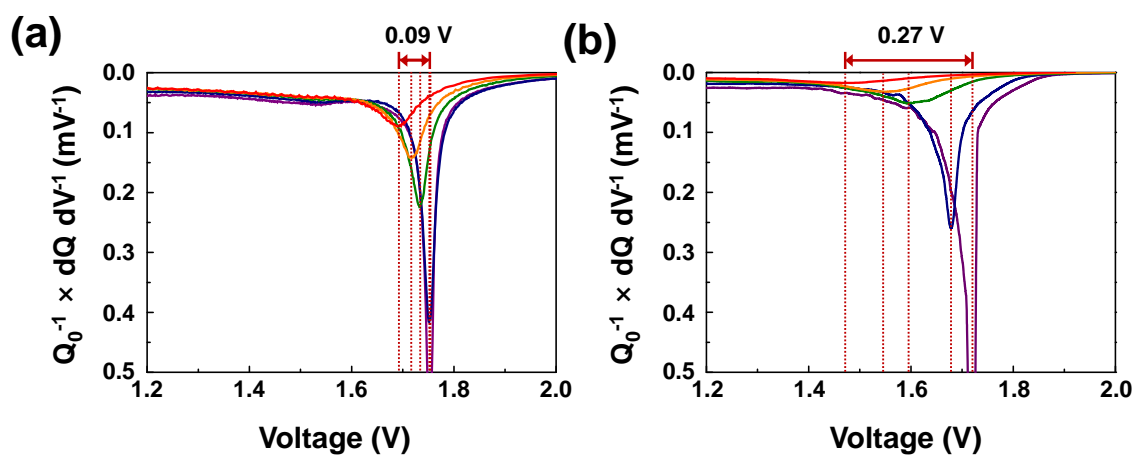


**Fig. S13** Differential capacities of (a) HTS and (b) C-TiO<sub>2</sub> anodes at various C-rates.



**Table S5.** Fitted Impedance Parameters of Nyquist Plots.

Active material	$R_s$ ( $\Omega$ )	$R_{ct}$ ( $\Omega$ )	$Q_y$ of $CPE_{pn}$ (mF)	$A_w^*$ ( $m\Omega s^{-0.5}$ )
HTS	3.29	119.1	42.6	0.4
C-TiO <sub>2</sub>	4.19	246.4	0.9	28.7

$$*A_w = RT/(n^2 F^2 A^2) (2/D)^{1/2} C.$$

where R is the gas constant, T is the temperature,  $n$  is the transferred electron number, A is the electrode area, D is the diffusion coefficient of  $Li^+$  in electrode and C is the concentration of  $Li^+$ .